The Akt1-eNOS Axis Illustrates the Specificity of Kinase-Substrate Relationships in Vivo

Michael Schleicher[1], **Jun Yu**[1], **Takahisa Murata**[2], **Berhad Derakhshan**[1], **Dimitriy Atochin**[3], **Li Qian**[3], **Satoshi Kashiwagi**[3], **Annarita Di Lorenzo**[1], **Kenneth D. Harrison**[1], **Paul L. Huang**[3,*], and **William C. Sessa**[1,*]

[1]Department of Pharmacology and Vascular Biology and Therapeutics Program, Amistad Building, Yale University School of Medicine, New Haven, CT 06520, USA.

[2]Department of Veterinary Pharmacology, Graduate School of Agriculture and Life Sciences, University of Tokyo, Bunkyo-ku, Tokyo 113-8657, Japan.

[3]Cardiovascular Research Center and Cardiology Division, Massachusetts General Hospital, Boston, MA 02129, USA.

Abstract

Akt1 is critical for many in vivo functions; however, the cell-specific substrates responsible remain to be defined. Here, we examine the importance of endothelial nitric oxide synthase (eNOS) as an Akt1 substrate by generating Akt1-deficient mice (Akt1$^{-/-}$ mice) carrying knock-in mutations (serine to aspartate or serine to alanine substitutions) of the critical Akt1 phosphorylation site on eNOS (serine 1176) that render the enzyme "constitutively active" or "less active." The eNOS mutations did not influence several phenotypes in Akt1$^{-/-}$ mice; however, the defective postnatal angiogenesis characteristic of Akt1$^{-/-}$ mice was rescued by crossing the Akt1$^{-/-}$ mice with mice carrying the constitutively active form of eNOS, but not by crossing with mice carrying the less active eNOS mutant. This genetic rescue resulted in the stabilization of hypoxia-inducible factor 1α (HIF-1α) and increased production of HIF-1α–responsive genes in vivo and in vitro. Thus, Akt1 regulates angiogenesis largely through phosphorylation of eNOS and NO-dependent signaling.

INTRODUCTION

Understanding the physiological importance of specific kinase-substrate relationships is difficult, especially for kinases that phosphorylate multiple substrates and for substrates that are phosphorylated on a single site by multiple kinases. For example, the kinase Akt1 phosphorylates multiple substrates, such as forkhead transcription factors and glycogen synthase kinase-3β (GSK-3β), on serine or threonine residues, several of which have been linked to cell survival, growth, and morphogenesis (1, 2). In turn, the Akt substrate endothelial nitric oxide synthase (eNOS) can be phosphorylated on serine 1176 (S^{1176}; murine isoform) by multiple kinases, including Akt, AMPK [adenosine monophosphate (AMP)–activated protein kinase], PKA [protein kinase A; also known as cyclic AMP (cAMP)–dependent protein kinase], PKG [guanosine 3′,5′-monophosphate (cGMP)– dependent protein kinase], and PKC (protein kinase C) (3). Biochemical and cellular evidence supporting the functional role of kinase-substrate pairs has led to a plethora of overlapping patterns of signaling pathways involving Akt, yet little is known about the relative importance of specific kinase-substrate pairs in vivo.

Angiogenesis is the process of formation of new blood vessels from existing structures that occurs during development and can be elicited postnatally by pathological events such as wounding or tissue ischemia (4). Akt1 is an important regulator of cardiovascular homeostasis, including such pathophysiological angiogenesis (5, 6). The multitude of Akt1 downstream partners and their described effects on various cellular functions allows broad speculation about the underlying mechanisms of how Akt1 functions in most mammalian cells including endothelial cells (ECs). For instance, Akt1 could influence angiogenesis by regulating EC survival through inhibition of caspase-9 (7) and BAD (Bcl-2–Bcl-XL– associated death promoter) (8, 9), cell growth through TSC2 (tuberous sclerosis complex protein 2) and mTORC1 (mammalian target of rapamycin complex 1) (10), metabolism through GSK-3b (11), proliferation through inhibition of p21 and p27 (12, 13), migration through girdin (14), or through a combination of any of the described pathways (2). Additionally, Akt1 can phosphorylate eNOS and thereby promote NO production (15, 16), thus enhancing blood flow, cell survival, morphogenesis, and angiogenesis in the setting of ischemia (17, 18).

Even though both Akt1 and eNOS are important regulators of pathophysiological angiogenesis, the in vivo relevance of this kinase-substrate relationship has not been unequivocally demonstrated and the possible involvement of multiple Akt1 targets in this process cannot be eliminated. Here, using a previously undescribed genetic strategy, we show that eNOS phosphorylation on the canonical Akt site, S^{1176}, is critical for many of the vascular actions of Akt in vivo.

RESULTS

Akt1-knockout mice expressing gain- and loss-of-function eNOS alleles reveal the importance of eNOS as an Akt1 substrate

To investigate the relevance of eNOS as a specific Akt1 target, we created genetically altered knock-in mice (fig. S1, A and B) in which the endogenous eNOS gene was replaced

with a mutated gene encoding a version of eNOS that either mimicked or abolished phosphorylation at the Akt1 phosphorylation site (S^{1176} replaced with aspartate, S1176D, or S^{1176} replaced with alanine, S1176A, respectively) (16). Expression of the mutated gene is regulated by the endogenous eNOS promoter, so that it should show perfect fidelity of expression and preserve all of the nuances of regulation of the native eNOS gene. The knock-in approach eliminates the possible confounding factors of gene copy number or insertion site effects inherent in transgenic approaches. The eNOS phosphomutant knock-in mice were bred to mice with an Akt1-null background (19) to generate the following strains: S1176D/Akt1$^{-/-}$ mice and S1176A/Akt1$^{-/-}$ mice (fig. S1C).

To validate these mice as a system for examining eNOS function, we checked the amount of phosphorylated eNOS (S^{1176}) in mouse lungs after systemic administration of vascular endothelial growth factor (VEGF) or phosphate-buffered saline (PBS). Basal and stimulated eNOS S^{1176} phosphorylation was reduced by more than 50% in Akt1-deficient mice (Akt1$^{-/-}$) compared to wild type (WT) and was undetectable in the phosphomutant, Akt1$^{-/-}$ mice (Fig. 1, A and B). En face staining of endothelium from carotid arteries for eNOS and phosphorylated eNOS S^{1176} showed that the localization and abundance of S1176D and S1176A eNOS was similar to that of eNOS in WT or Akt1$^{-/-}$ mice (Fig. 1C). However, acetylcholine (ACh)–induced cGMP production, a surrogate for NO production, was decreased in aortic rings from Akt1$^{-/-}$ and S1176A/Akt1$^{-/-}$ mice compared to WT mice, whereas the S1176D/Akt1$^{-/-}$ animals showed a marked increase in basal cGMP production compared to WT mice (Fig. 1D). Similar data were obtained by measuring NO production (assayed as the stable breakdown product nitrite, NO_2^-) in mouse lung endothelial cells (MLECs) isolated from these strains (fig. S2A), where basal and A23187-stimulated NO_2^- accumulation (for 30-min accumulation) was reduced in Akt1$^{-/-}$ cells; effects that were rescued in S1176D/Akt1$^{-/-}$ but not S1176A/Akt1$^{-/-}$ cells. In addition, after 6 hours of incubation, basal accumulation of NO_2^- was markedly increased in S1176D/Akt1$^{-/-}$ cells compared to WT (fig. S2B). These data show that Akt1 is necessary for most of eNOS phosphorylation on S^{1176} and NO release in vivo and that mutation of eNOS S^{1176} to aspartate enables its production of NO (20) despite the loss of endogenous Akt1.

eNOS S^{1176} phosphorylation status does not affect the growth or fertility of Akt1$^{-/-}$ mice, but does influence cell survival

Because Akt1 can phosphorylate multiple substrates and regulate multiple cellular functions, we examined Akt1 substrate phosphorylation in ECs isolated from the different strains of mice. Loss of Akt1 decreased the phosphorylation of GSK-3β and Mdm-2, but not that of FoxO1 (forkhead box O1); however, the expression of mutant eNOS in the Akt1-null background did not appear to influence the total or phosphorylated amounts of these substrates (Fig. 2A). As is typical (21), Akt1-null cells showed decreased cell proliferation, a phenotype that could not be rescued by either mutant eNOS allele (Fig. 2B). Two other phenotypes characteristic of Akt1-null mice are reduction in body mass and smaller litter size (attributable to placental or maternal mam-mary defects) (19, 21). The presence of both eNOS alleles in the Akt1-null background did not affect either of these phenotypes (Fig. 2, C and D). Loss of Akt1 promoted apoptosis [assessed by an increase in TUNEL (terminal deoxynucleotidyl transferase–mediated deoxyuridine triphosphate nick end labeling)-

positive nuclei] in the endothelium of isolated aortae (Fig. 2, E and F), consistent with Akt1's well-known prosurvival function (2); S1176D eNOS slightly reduced EC apoptosis, consistent with the role of NO in promoting cell survival of ECs (3). These data suggest that Akt1 substrates other than eNOS mediate multiple phenotypes (decreased cell growth, body mass, and litter size and increased apoptosis) associated with Akt1 deficiency.

eNOS is a critical Akt substrate for pathological angiogenesis

We used wound healing assays to investigate the role of eNOS as a downstream target of Akt1 in postnatal, pathological angiogenesis. Wound healing–evoked angiogenesis is impaired in Akt1 knockout mice (6) and, consistent with impaired angiogenesis, the time to complete healing was delayed in Akt1-null mice. This delay was prolonged in S1176A/Akt1$^{-/-}$ mice but was restored to the WT duration in S1176D/Akt1$^{-/-}$ mice (Fig. 3A). Quantification of ECs with endothelial-specific isolectin B4 staining revealed that revascularization was impaired after 4 days in Akt1$^{-/-}$ and S1176A/Akt1$^{-/-}$ mice but was comparable to that of WT in S1176D/Akt1$^{-/-}$ animals (Fig. 3, B and C). This suggests that eNOS is downstream of Akt1 in wound-healing angiogenesis.

In a second model of adaptive angiogenesis, we subjected mice to femoral artery ligation, thereby inducing ischemia in the lower leg. eNOS phosphorylation was decreased in ischemic muscle tissue of Akt1$^{-/-}$ mice compared to that of WT animals (fig. S3). As previously described (5), Akt1 knockout mice, unlike WT animals, did not recover blood flow to the lower limb within 4 weeks, resulting in severe necrosis of the ischemic tissue and eventual loss of the lower limb (Fig. 4, A to C) (5). Staining for isolectin B4 (Fig. 4, D and E) and smooth muscle α-actin (as a marker for pericytes, Fig. 4, F and G) revealed that failure to recover blood flow is caused by the lack of revascularization within the ischemic tissue and by impaired pericyte recruitment, which occurs with angiogenic blood vessel maturation. In the S1176D/Akt1$^{-/-}$ mice, however, blood flow recovery, clinical score, revascularization, and pericyte recruitment were all comparable to that of WT mice (Fig. 4, A to G). The S1176A/Akt1$^{-/-}$ mice did not have a more severe phenotype than did the Akt1$^{-/-}$ mice, suggesting that, in the setting of hind-limb ischemia, Akt1 is the main kinase that phosphorylates eNOS on S^{1176}. The restoration of wound angiogenesis and revascularization after ischemic injury by phosphomimetic eNOS supports the idea that the phosphorylation of eNOS on S^{1176} is the main pathway through which Akt1 acts in pathophysiological angiogenesis.

The abundance of HIF-1α, but not that of PGC-1α, is regulated by the Akt1-eNOS axis

Deprivation of oxygen and nutrients during ischemia triggers an angiogenic response, including increased production of angiogenic factors such as VEGF and up-regulation of its receptors (4). In most ischemic scenarios, the stabilization and activation of hypoxia-inducible factor 1α (HIF-1α) promotes many aspects of this angiogenic response, such as enhancing VEGF production (22). However, a recent study suggests that activation of the transcriptional coactivator PGC-1α [peroxisome proliferator–activated receptor γ (PPARγ) coactivator 1α], rather than the stabilization of HIF-1α, triggers the production of VEGF after ischemia and that genetic ablation of PGC-1α results in impaired recovery of blood flow (23). Thus, both HIF-1α and PGC-1α can regulate ischemic revascularization. To see

whether HIF-1α– or PGC-1α–dependent pathways or both are involved in the eNOS-mediated rescue of the Akt1$^{-/-}$ phenotype, we elicited hind-limb ischemia in all four strains of mice and isolated messenger RNA (mRNA) from the gastrocnemius muscle 6 and 24 hours after ischemia. Quantitative polymerase chain reaction (PCR) analysis revealed that the expression of a set of HIF-1α–responsive genes, including those encoding VEGF-A, VEGF receptor (Flk-1), and angiopoietin-like 4 protein (Angptl-4), was increased in WT mice after ischemic injury. This increase in mRNA was not apparent in Akt1$^{-/-}$ and S1176A/Akt1$^{-/-}$ mice but was present in S1176D/Akt1$^{-/-}$ mice (Fig. 5A). Next, we quantified HIF-1α protein abundance in ischemic gastrocnemius muscle extracts by enzyme-linked immunosorbent assay (ELISA). We found that, whereas HIF-1α was detectable after ischemia in WT and S1176D/Akt1$^{-/-}$ mice, it was not detectable (n.d.) in Akt1$^{-/-}$ or S1176A/Akt1$^{-/-}$ mice or in the contralateral, nonischemic muscles of WT and S1176D/Akt1$^{-/-}$ mice (Fig. 5B).

As reported recently (23), PGC-1α mRNA abundance increased after ischemia in WT mice (fig. S4A) and, like HIF-1α, this increase was absent in Akt1$^{-/-}$ knockout mice. Unlike the HIF-1α–responsive genes, the abundance of PGC-1α mRNA remained low in S1176D/Akt1$^{-/-}$ mice. Although there were differences in the effects of ischemia on mRNA abundance of the HIF-1α–responsive genes in Akt1$^{-/-}$ and S1176A/Akt1$^{-/-}$ mice, all four strains showed equal changes in the expression of HSP-70 and HSP-90, which are hallmarks of ischemic stress (fig. S4B). These data support the model that constitutively active eNOS rescues the functional and molecular phenotypes observed in Akt1$^{-/-}$ mice to promote angiogenesis.

These in vivo results suggest that Akt1 regulates the HIF-1α–mediated angiogenic response through activation of eNOS and subsequent increases in NO. To further investigate this possibility, we performed in vitro experiments using ECs isolated from WT or Akt1-null mice. Hypoxia (0.5%) increased the mRNA abundance of the HIF-1α–responsive genes VEGF-A, glucose transporter 1 (GLUT-1), and ANGptl-4 in WT but not in Akt1$^{-/-}$ cells (Fig. 5C). Hypoxic gene induction in WT cells could be partially inhibited by incubation with the NOS inhibitor N^{G}-nitro-L-arginine (L-NNA) and responses to hypoxia could be elicited in Akt1$^{-/-}$ cells incubated with the NO donor (Z)-1-[2-(2-aminoethyl)-N-(2-ammonioethyl)amino]diazen-1-ium-1,2-diolate (DETA-NONOate). Changes in HIF-1α protein abundance measured by Western blot (Fig. 5, D and E) correlated with the changes in VEGF-A, GLUT-1, and ANGptl-4 mRNA and DETA-NONOate increased HIF-1α abundance in hypoxic Akt1$^{-/-}$ cells. Thus, the in vitro data support the idea that Akt1 regulates HIF-1α stability through activation of eNOS and thereby triggers the angiogenic response.

Several potential mechanisms exist for how NO regulates HIF-1α abundance

Next, we investigated how NO may influence HIF-1α protein stability. HIF-1α can itself be posttranslationally modified by NO through S-nitrosylation, thereby stabilizing HIF (24). Therefore, we performed a biotin switch assay for nitrosylated proteins (25) in WT and Akt1$^{-/-}$ ECs under normoxic and hypoxic conditions. We could not detect nitrosylation of HIF-1α protein, even though eNOS was nitrosylated [fig. S5A (26)].

Reactive oxygen species (ROS) have also been implicated as playing a role in HIF-1α stabilization (27, 28). Because NO can increase intracellular ROS through inhibition of cytochrome c oxidase and subsequent uncoupling of the respiratory chain, we checked whether alteration of intracellular ROS concentrations affected the degree of HIF-1α–responsive gene expression. However, we could not detect differences in induction of HIF-1α–responsive genes in WT or Akt1$^{-/-}$ cells in the presence of two ROS scavengers, TEMPOL and pegylated catalase (PEG-CAT), or of the superoxide donor pyrogallol (fig. S5B).

Finally, we determined whether alterations of prolyl hydroxylase (PHD) activity could explain the mechanism of NO-dependent HIF-1α stabilization (29). The prolyl hydroxylation of HIF-1α is necessary for the ubiquitin-dependent degradation of this transcription factor; thus, a reduction in PHD activity may enhance HIF-1α abundance, leading to increased HIF-1α–dependent gene expression. We found that treatment of WT and Akt1$^{-/-}$ ECs with the PHD inhibitor dimethyloxaloylglycine (DMOG) increased HIF-1α–dependent gene induction in a similar manner in both WT and Akt1$^{-/-}$ ECs (fig. S5C).

DISCUSSION

This study shows that despite the growing list of possible substrates for Akt1, phosphorylation of eNOS on S^{1176} appears critical for the actions of Akt in promoting angiogenesis. Genetic loss of either eNOS or Akt1 does not affect embryonic vascular development but leads to impaired ischemic angiogenesis and wound healing (5, 6, 18, 30); here, we show that introduction of S1176D eNOS mimicking a "gain of function," but not S1176A eNOS, rescues the impairment in angiogenesis seen in Akt1-deficient mice. Because other kinases (AMPK, PKA, and PKG) that phosphorylate eNOS on S^{1176} are presumably active in Akt1$^{-/-}$ mice, the allele-specific rescue of the Akt1$^{-/-}$ phenotypes by the "phospho-" versus "dephospho-" status of S^{1176} implies the critical importance of Akt1 and this residue in limb recovery and wound healing. To our knowledge, this is a rare instance in which a highly specific relationship between a particular kinase and substrate can be identified in a complex in vivo system.

Previous studies identifying critical roles of specific Akt substrates in biological processes have relied on overexpression, dominant-negative strategies, and knockdown approaches in cultured cells, as well as genetic knockouts of individual Akt isoforms and specific point mutations of key substrates in vivo (2, 31). Most Akt1 substrates are expressed in all mammalian cells, whereas eNOS is specifically expressed in ECs; thus, the coupling of Akt1 to eNOS provided a model in which to investigate the specificity of kinase-substrate relationship.

In intact lung tissues, we found that treatment with VEGF increased eNOS phosphorylation on S^{1176} and that this was reduced, but not eliminated, in Akt1$^{-/-}$ mice, arguing that indeed other kinases contribute to eNOS phosphorylation at this site. However, this residual phosphorylation in Akt1$^{-/-}$ mice was not sufficient to promote blood flow recovery and tissue healing, arguing that Akt phosphorylation of eNOS plays a critical role in adaptive angiogenesis. The roles of Akt in pathophysiological angiogenesis appear temporally

distinct; Akt 1 is necessary for protection against atherosclerosis, ischemic angiogenesis, and wound healing (5, 6, 32, 33), but in models where Akt is persistently activated (using myristoylated and constitutively activated Akt), Akt signaling may promote cell senescence, enhance vascular leakage, and retard or promote angiogenesis through an apparently eNOS-independent, rapamycin-sensitive pathway (34–36). Our results in wound healing and limb ischemia point toward eNOS being downstream of Akt in these more acute models; however, additional experiments are required to uncover the substrates responsible for phenotypes after sustained Akt activation.

In our studies in ischemic tissue in vivo and in cultured ECs, Akt1 seems to be required for HIF-1α stabilization and the activation of its target genes by means of eNOS-derived NO. The idea that Akt regulates HIF-1α signaling in cancer is accepted (37–40), and this relationship has begun to emerge in ischemic settings as well (41). The effects of NO on HIF-1α stability have been intensely investigated. NO can either stabilize or destabilize HIF-1α depending on the cells, the duration and degree of hypoxia, and mitochondrial function (29, 42–45). At least three putative mechanisms may explain this effect: NO may directly modify HIF-1α through nitrosylation; NO may increase ROS, which stabilize HIF-1α; and NO may inhibit HIF PHDs through NO binding the iron cofactor required for PHD activity (30). Our results with cultured ECs support the idea that NO may inhibit PHD activity, because we could not detect nitrosylation of HIF-1α protein or identify an involvement of ROS; however, inhibition of PHD activity normalized differences in HIF-1α– dependent gene expression in WT and Akt1$^{-/-}$ ECs. However, it is feasible that all these mechanisms may operate in vivo.

In summary, our results provide an example of in vivo context-specific, kinase-substrate specificity. We found that eNOS was the predominant Akt substrate necessary for angiogenesis; however, it was less critical in promoting Akt-dependent growth, fertility and pregnancy, and survival. S1176D eNOS, but not S1176A eNOS, rescued the angiogenic phenotypes elicited by loss of Akt1, arguing against major roles of other Akt substrates, such as girdin, FoxO1, and GSK-3β, in the models investigated. Moreover, the other kinases that phosphorylate eNOS on S^{1176} do not appear to play a major role in the vivo systems used in our study. Mechanistically, we suggest that phosphorylation of eNOS at S^{1176} by Akt1 and the subsequent increase in NO production contributes to revascularization, in part, by preserving blood flow, and by stabilizing HIF-1α and thereby promoting HIF-1α– dependent gene expression or both. Such a dual function of eNOS-derived NO may explain the critical role of this pathway in postnatal angiogenesis.

MATERIALS AND METHODS

Materials

The HIF-1α ELISA kit was from R&D Systems. The Cell Death Detection kit was from Roche. The cGMP Biotrak Enzyme assay kit was from Amersham. VEGF was a gift from Genentec. Ceramide was from Calbiochem. DETA-NONOate, isolectin B4, L-NNA, isobutylmethylxantine (IBMX), ACh, and antibodies directed against β-actin and smooth muscle α-actin were from Sigma. Antibodies against HIF-1α and vascular endothelial

cadherin (VE-cadherin) were from Santa Cruz Biotechnology. Antibodies against eNOS and p-eNOS were from BD Transduction. All other antibodies were from Cell Signaling.

Isolation of MLECs

MLECs were isolated and immortalized as described before (5). Cell growth was analyzed by seeding equal numbers of cells per well and counting at indicated time points.

Generation of eNOS S1179A and S1179D knock-in mice

Knock-in mice carrying the S1176A and S1176D mutations in the endogenous eNOS locus were generated by homologous recombination. Within exon 26, the TCT codon for S^{1176} was replaced with GCT for the S1176A mutation and with GAT for the S1176D mutation. The targeting construct carries these mutations in exon 26, flanked by homologous regions on either side. It also includes a neomycin resistance gene adjacent to the mutation to allow positive selection. The neomycin resistance gene is flanked by lox P sites, facilitating its removal in one step by Cre recombinase. Although the eNOS gene does not have a typical polyadenylation site (AATAAA), it does have a potential alternative site (CATAAA). We avoided placing the neomycin resistance gene near this site. A thymidine kinase (TK) gene is incorporated at one end of the construct to allow negative selection; the TK gene is not incorporated into the genome.

Using J1 embryonic stem cells, we generated chimeric mice with germline transmission of these mutations. Mice were mated with EIIa-Cre transgenic mice to delete the neomycin resistance gene between the loxP sites. This leaves one copy of the loxP site and the targeted mutation (S1176D or S1176A). Once back-bred, eNOS S1176D or S1176A mice were bred to congenic Akt1-deficient mice (19) and littermates were used as WT controls.

eNOS phosphorylation in vivo

VEGF (80 μg per kilogram of body weight) was injected into 8- to 12-week-old male mice as described (46). After 5 min, the mice were perfused with cold PBS containing phosphatase inhibitors; the lungs were harvested, homogenized, and lysed in SDS–sample buffer and lysates were used for Western blot analysis.

En face staining of carotid arteries

Carotid arteries of 8- to12-week-old male mice were dissected, cut open, and pinned with surgical needles. Specimens were fixed with 4% paraformaldehyde (10 min, 4°C), permeabilized with 0.3% Triton X-100 [30 min, room temperature (RT)], and antigens were blocked in 5% fetal bovine serum (FBS) (30 min, RT). After incubation with primary (rabbit antibody against eNOS and mouse antibody against phospho-eNOS) and secondary antibodies, specimens were analyzed by indirect immunofluorescence.

cGMP production assays from aortae

Aortae from 8- to 12-week-old male mice were dissected, freed from fat, and cut into 1- to 2-mm pieces and placed into Dulbecco's modified Eagle's medium (DMEM) containing antibiotics for 3 hours. Afterwards, aortic pieces were stimulated for 5 min with 1 μM ACh (to elicit increases in cGMP) in the presence of the phosphodiesterase inhibitor IBMX (200

μM), snap-frozen in liquid nitrogen, and homogenized. Preincubation with IBMX was used to inhibit phosphodiesterase activity, thus allowing for quantification of cGMP accumulation under various conditions. All values shown were calculated by taking the original value and subtracting the average of the control groups that were pretreated with IBMX and the NOS inhibitor ʟ-NNA and stimulated with ACh. Thus, we measure NOS-dependent increases in cGMP as a surrogate for eNOS activation. Homogenates were processed according to the manufacturer's protocol (cGMP Enzymeimmunoassay Biotrak System, Amersham).

En face TUNEL assay

Aortas of 8- to 12-week-old male mice were dissected, cut into 1- to 3-mm pieces, and rinsed with DMEM, and apoptosis was stimulated with 50 μM ceramide for 16 hours. Afterwards, pieces were cut open and pinned with surgical needles. Specimens were fixed with 4% paraformaldehyde (10 min, 4°C) and permeabilized with 0.3% Triton X-100 (30 min, RT), and antigens were blocked in 5% FBS (30 min, RT). Specimens were stained for VE-cadherin and apoptotic nuclei with the Cell Death Detection kit (Roche).

Wound healing assays

Twelve-week-old male mice were anesthetized and two wounds (6-mm diameter) were punched into the back skin. Wound size was monitored until complete closure. For assessing wound angiogenesis, mice were killed after 4 days; wounded skin was excised, fixed in 4% paraformaldehyde, paraffin-embedded, and sectioned, and ECs were stained with isolectin B4 and analyzed by indirect immunofluorescence.

Hind-limb ischemia assays

Hind-limb ischemia assays and analysis of the angiogenic response in the ischemic muscle sections were carried out as described (5, 18). Blood flow was measured with a deep penetrating laser Doppler and the following clinical scoring system was used to discern the extent of tissue ischemia: 0, normal appearance; 1, reddish foot; 2, black toes present; 3, necrotic muscle tissue present; 4, >50% of the foot is necrotic; 5, complete foot necrosis.

Quantitative reverse transcription PCR analysis

Samples from tissue or cell culture were resuspended and homogenized with Trizol. Total RNA was isolated with the RNAEasy kit (Qiagen) and transcribed into complementary DNA with the use of the TaqMan protocol (Applied Biosystems). Quantitative PCRs were carried out on an iCycler (Biorad) with specific primers against the genes of interest, SYBRgreen (Biorad) ready mix.

Analysis of HIF-1α protein

HIF-1α protein abundance from muscle homogenates was determined by specific ELISA with the DuoSet IC kit (R&D Systems). HIF-1α protein abundance from cell lysates was analyzed by Western blot and subsequent quantification by ImageJ Software.

Statistical analysis

Data are expressed as mean ± SEM. Statistical significance was determined by one-way or two-way analysis of variance (ANOVA) followed by a Bonferroni's *t* test for multiple comparisons or by a Student's *t* test with the GraphPad (San Diego) Prism software.

Supplementary Material

Refer to Web version on PubMed Central for supplementary material.

Acknowledgments

REFERENCES

1. Fayard E, Tintignac LA, Baudry A, Hemmings BA. Protein kinase B/Akt at a glance. J. Cell Sci. 2005; 118:5675–5678. [PubMed: 16339964]

2. Manning BD, Cantley LC. AKT/PKB signaling: Navigating downstream. Cell. 2007; 129:1261–1274. [PubMed: 17604717]

3. Sessa WC. eNOS at a glance. J. Cell Sci. 2004; 117:2427–2429. [PubMed: 15159447]

4. Carmeliet P. Angiogenesis in health and disease. Nat. Med. 2003; 9:653–660. [PubMed: 12778163]

5. Ackah E, Yu J, Zoellner S, Iwakiri Y, Skurk C, Shibata R, Ouchi N, Easton RM, Galasso G, Birnbaum MJ, Walsh K, Sessa WC. Akt1/protein kinase Bα is critical for ischemic and VEGF-mediated angiogenesis. J. Clin. Invest. 2005; 115:2119–2127. [PubMed: 16075056]

6. Somanath PR, Chen J, Byzova TV. Akt1 is necessary for the vascular maturation and angiogenesis during cutaneous wound healing. Angiogenesis. 2008; 11:277–288. [PubMed: 18415691]

7. Cardone MH, Roy N, Stennicke HR, Salvesen GS, Franke TF, Stanbridge E, Frisch S, Reed JC. Regulation of cell death protease caspase-9 by phosphorylation. Science. 1998; 282:1318–1321. [PubMed: 9812896]

8. Datta SR, Dudek H, Tao X, Masters S, Fu H, Gotoh Y, Greenberg ME. Akt phosphorylation of BAD couples survival signals to the cell-intrinsic death machinery. Cell. 1997; 91:231–241. [PubMed: 9346240]

9. del Peso L, González-García M, Page C, Herrera R, Nunez G. Interleukin-3-induced phosphorylation of BAD through the protein kinase Akt. Science. 1997; 278:687–689. [PubMed: 9381178]

10. Potter CJ, Pedraza LG, Xu T. Akt regulates growth by directly phosphorylating Tsc2. Nat. Cell Biol. 2002; 4:658–665. [PubMed: 12172554]

11. Cross DA, Alessi DR, Cohen P, Andjelkovich M, Hemmings BA. Inhibition of glycogen synthase kinase-3 by insulin mediated by protein kinase B. Nature. 1995; 378:785–789. [PubMed: 8524413]

12. Liang J, Zubovitz J, Petrocelli T, Kotchetkov R, Connor MK, Han K, Lee J-H, Ciarallo S, Catzavelos C, Beniston R, Franssen E, Slingerland JM. PKB/Akt phosphorylates p27, impairs nuclear import of p27 and opposes p27-mediated G_1 arrest. Nat. Med. 2002; 8:1153–1160. [PubMed: 12244302]

13. Zhou BP, Liao Y, Xia W, Spohn B, Lee MH, Hung MC. Cytoplasmic localization of p21[Cip1/WAF1] by Akt-induced phosphorylation in *HER-2/neu*-overexpressing cells. Nat. Cell Biol. 2001; 3:245–252. [PubMed: 11231573]

14. Kitamura T, Asai N, Enomoto A, Maeda K, Kato T, Ishida M, Jiang P, Watanabe T, Usukura J, Kondo T, Constantini F, Murohara T, Takahashi M. Regulation of VEGF-mediated angiogenesis by the Akt/PKB substrate Girdin. Nat. Cell Biol. 2008; 10:329–337. [PubMed: 18264090]

15. Dimmeler S, Fleming I, Fisslthaler B, Hermann C, Busse R, Zeiher AM. Activation of nitric oxide synthase in endothelial cells by Akt-dependent phosphorylation. Nature. 1999; 399:601–605. [PubMed: 10376603]

16. Fulton D, Gratton JP, McCabe TJ, Fontana J, Fujio Y, Walsh K, Franke TF, Papapetropoulos A, Sessa WC. Regulation of endothelium-derived nitric oxide production by the protein kinase Akt. Nature. 1999; 399:597–601. [PubMed: 10376602]

17. Atochin DN, Wang A, Liu VW, Critchlow JD, Dantas AP, Looft-Wilson R, Murata T, Salomone S, Shin HK, Ayata C, Moskowitz MA, Michel T, Sessa WC, Huang PL. The phosphorylation state of eNOS modulates vascular reactivity and outcome of cerebral ischemia in vivo. J. Clin. Invest. 2007; 117:1961–1967. [PubMed: 17557122]

18. Yu J, deMuinck ED, Zhuang Z, Drinane M, Kauser K, Rubanyi GM, Qian HS, Murata T, Escalante B, Sessa WC. Endothelial nitric oxide synthase is critical for ischemic remodeling, mural cell recruitment, and blood flow reserve. Proc. Natl. Acad. Sci. U.S.A. 2005; 102:10999–11004. [PubMed: 16043715]

19. Cho H, Thorvaldsen JL, Chu Q, Feng F, Birnbaum MJ. Akt1/PKBa is required for normal growth but dispensable for maintenance of glucose homeostasis in mice. J. Biol. Chem. 2001; 276:38349–38352. [PubMed: 11533044]

20. McCabe TJ, Fulton D, Roman LJ, Sessa WC. Enhanced electron flux and reduced calmodulin dissociation may explain "calcium-independent" eNOS activation by phosphorylation. J. Biol. Chem. 2000; 275:6123–6128. [PubMed: 10692402]

21. Fernández-Hernando C, Ackah E, Yu J, Suarez Y, Murata T, Iwakiri Y, Prendergast J, Miao RQ, Birnbaum MJ, Sessa WC. Loss of Akt1 leads to severe atherosclerosis and occlusive coronary artery disease. Cell Metab. 2007; 6:446–457. [PubMed: 18054314]

22. Hickey MM, Simon MC. Regulation of angiogenesis by hypoxia and hypoxiainducible factors. Curr. Top. Dev. Biol. 2006; 76:217–257. [PubMed: 17118268]

23. Arany Z, Foo SY, Ma Y, Ruas JL, Bommi-Reddy A, Girnun G, Cooper M, Laznik D, Chinsomboon J, Rangwala SM, Baek KH, Rosenzweig A, Spiegelman BM. HIF-independent regulation of VEGF and angiogenesis by the transcriptional coactivator PGC-1α. Nature. 2008; 451:1008–1012. [PubMed: 18288196]

24. Li F, Sonveaux P, Rabbani ZN, Liu S, Yan B, Huang Q, Vujaskovic Z, Dewhirst MW, Li CY. Regulation of HIF-1α stability through S-nitrosylation. Mol. Cell. 2007; 26:63–74. [PubMed: 17434127]

25. Hao G, Derakhshan B, Shi L, Campagne F, Gross SS. SNOSID, a proteomic method for identification of cysteine S-nitrosylation sites in complex protein mixtures. Proc. Natl. Acad. Sci. U.S.A. 2006; 103:1012–1017. [PubMed: 16418269]

26. Erwin PA, Lin AJ, Golan DE, Michel T. Receptor-regulated dynamic S-nitrosylation of endothelial nitric-oxide synthase in vascular endothelial cells. J. Biol. Chem. 2005; 280:19888–19894. [PubMed: 15774480]

27. Chandel NS, McClintock DS, Feliciano CE, Wood TM, Melendez JA, Rodriguez AM, Schumacker PT. Reactive oxygen species generated at mitochondrial complex III stabilize hypoxia-inducible factor-1α during hypoxia: A mechanism of O_2 sensing. J. Biol. Chem. 2000; 275:25130–25138. [PubMed: 10833514]

28. López-Lázaro M. HIF-1: Hypoxia-inducible factor or dysoxia-inducible factor? FASEB J. 2006; 20:828–832. [PubMed: 16675839]

29. Metzen E, Zhou J, Jelkmann W, Fandrey J, Brüne B. Nitric oxide impairs normoxic degradation of HIF-1α by inhibition of prolyl hydroxylases. Mol. Biol. Cell. 2003; 14:3470–3481. [PubMed: 12925778]

30. Murohara T, Asahara T, Silver M, Bauters C, Masuda H, Kalka C, Kearney M, Chen D, Symes JF, Fishman MC, Huang PL, Isner JM. Nitric oxide synthase modulates angiogenesis in response to tissue ischemia. J. Clin. Invest. 1998; 101:2567–2578. [PubMed: 9616228]

31. Bayascas JR, Sakamoto K, Armit L, Arthur JS, Alessi DR. Evaluation of approaches to generation of tissue-specific knock-in mice. J. Biol. Chem. 2006; 281:28772–28781. [PubMed: 16887794]

32. Mukai Y, Rikitake Y, Shiojima I, Wolfrum S, Satoh M, Takeshita K, Hiroi Y, Salomone S, Kim HH, Benjamin LE, Walsh K, Liao JK. Decreased vascular lesion formation in mice with inducible endothelial-specific expression of protein kinase Akt. J. Clin. Invest. 2006; 116:334–343. [PubMed: 16453020]

33. Shiojima I, Walsh K. Role of Akt signaling in vascular homeostasis and angiogenesis. Circ. Res. 2002; 90:1243–1250. [PubMed: 12089061]

34. Chen J, Somanath PR, Razorenova O, Chen WS, Hay N, Bornstein P, Byzova TV. Akt1 regulates pathological angiogenesis, vascular maturation and permeability in vivo. Nat. Med. 2005; 11:1188–1196. [PubMed: 16227992]

35. Phung TL, Ziv K, Dabydeen D, Eyiah-Mensah G, Riveros M, Perruzzi C, Sun J, Monahan-Earley RA, Shiojima I, Nagy JA, Lin MI, Walsh K, Dvorak AM, Briscoe DM, Neeman M, Sessa WC, Dvorak HF, Benjamin LE. Pathological angiogenesis is induced by sustained Akt signaling and inhibited by rapamycin. Cancer Cell. 2006; 10:159–170. [PubMed: 16904613]

36. Wang CY, Kim HH, Hiroi Y, Sawada N, Salomone S, Benjamin LE, Walsh K, Moskowitz MA, Liao JK. Obesity increases vascular senescence and susceptibility to ischemic injury through chronic activation of Akt and mTOR. Sci. Signal. 2009; 2:ra11. [PubMed: 19293429]

37. Hudson CC, Liu M, Chiang GG, Otterness DM, Loomis DC, Kaper F, Giaccia AJ, Abraham RT. Regulation of hypoxia-inducible factor 1a expression and function by the mammalian target of rapamycin. Mol. Cell. Biol. 2002; 22:7004–7014. [PubMed: 12242281]

38. Majumder PK, Febbo PG, Bikoff R, Berger R, Xue Q, McMahon LM, Manola J, Brugarolas J, McDonnell TJ, Golub TR, Loda M, Lane HA, Sellers WR. mTOR inhibition reverses Akt-dependent prostate intraepithelial neoplasia through regulation of apoptotic and HIF-1-dependent pathways. Nat. Med. 2004; 10:594–601. [PubMed: 15156201]

39. Mazure NM, Chen EY, Laderoute KR, Giaccia AJ. Induction of vascular endothelial growth factor by hypoxia is modulated by a phosphatidylinositol 3-kinase/Akt signaling pathway in Ha-*ras*-transformed cells through a hypoxia inducible factor-1 transcriptional element. Blood. 1997; 90:3322–3331. [PubMed: 9345014]

40. Rankin EB, Giaccia AJ. The role of hypoxia-inducible factors in tumorigenesis. Cell Death Differ. 2008; 15:678–685. [PubMed: 18259193]

41. Li L, Qu Y, Mao M, Xiong Y, Mu D. The involvement of phosphoinositid 3-kinase/Akt pathway in the activation of hypoxia-inducible factor-1α in the developing rat brain after hypoxia-ischemia. Brain Res. 2008; 1197:152–158. [PubMed: 18241842]

42. Callapina M, Zhou J, Schmid T, Köhl R, Brüne B. NO restores HIF-1α hydroxylation during hypoxia: Role of reactive oxygen species. Free Radic. Biol. Med. 2005; 39:925–936. [PubMed: 16140212]

43. Hagen T, Taylor CT, Lam F, Moncada S. Redistribution of intracellular oxygen in hypoxia by nitric oxide: Effect on HIF1α. Science. 2003; 302:1975–1978. [PubMed: 14671307]

44. Mansfield KD, Guzy RD, Pan Y, Young RM, Cash TP, Schumacker PT, Simon MC. Mitochondrial dysfunction resulting from loss of cytochrome c impairs cellular oxygen sensing and hypoxic HIF-α activation. Cell Metab. 2005; 1:393–399. [PubMed: 16054088]

45. Berchner-Pfannschmidt U, Yamac H, Trinidad B, Fandrey J. Nitric oxide modulates oxygen sensing by hypoxia-inducible factor 1-dependent induction of prolyl hydroxylase 2. J. Biol. Chem. 2007; 282:1788–1796. [PubMed: 17060326]

46. Bauer PM, Yu J, Chen Y, Hickey R, Bernatchez PN, Looft-Wilson R, Huang Y, Giordano F, Stan RV, Sessa WC. Endothelial-specific expression of caveolin-1 impairs microvascular permeability and angiogenesis. Proc. Natl. Acad. Sci. U.S.A. 2005; 102:204–209. [PubMed: 15615855]
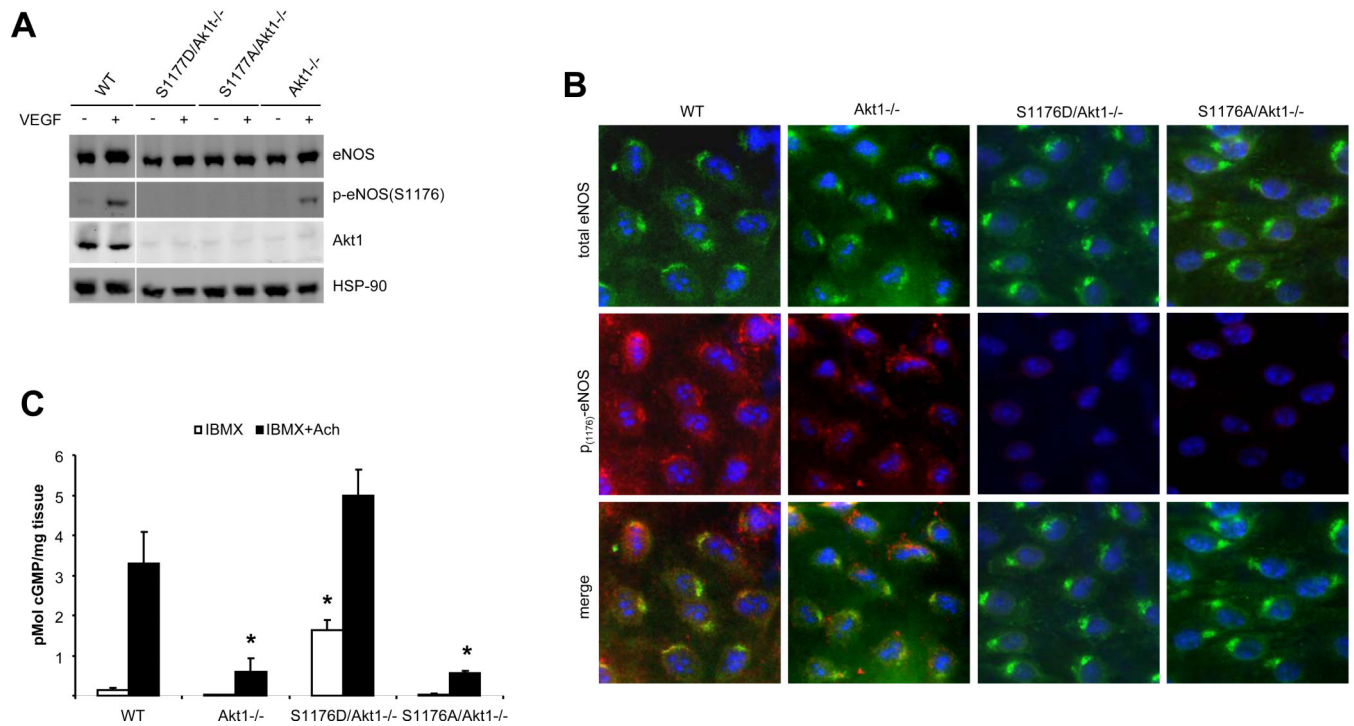
Fig. 1.

Characterization of eNOS status in mutant mice. (A) Wild-type (WT), Akt1-null (Akt1$^{-/-}$), activated, phosphomimetic eNOS mice lacking Akt1 (S1176D/Akt1$^{-/-}$), and nonphosphorylatable eNOS mice lacking Akt1 (S1176A/Akt1$^{-/-}$) received injections of VEGF through the jugular vein. Samples were analyzed by Western blotting for eNOS, phospho-eNOS (p-eNos, S^{1176}), Akt1, and HSP-90 proteins and (B) the relative ratio of p-eNOS (S^{1176}) to total eNOS was quantified (n = 3 mice per group). (C) En face immunofluorescent staining of carotid arteries for total eNOS (green, top), p-eNOS (1176) (red, middle), and merged images [blue, DAPI (4′,6-diamidino-2-phenylindole), bottom]. (D) cGMP assays were performed on aortic rings pretreated with IBMX and stimulated with ACh (1 μM, black bars) or vehicle (control, white bars). In (B) and (D), error bars indicate SEM; *P < 0.05 compared to control, ^{+}P < 0.05 compared to WT stimulated, and **P compared to WT basal using a two-way ANOVA.
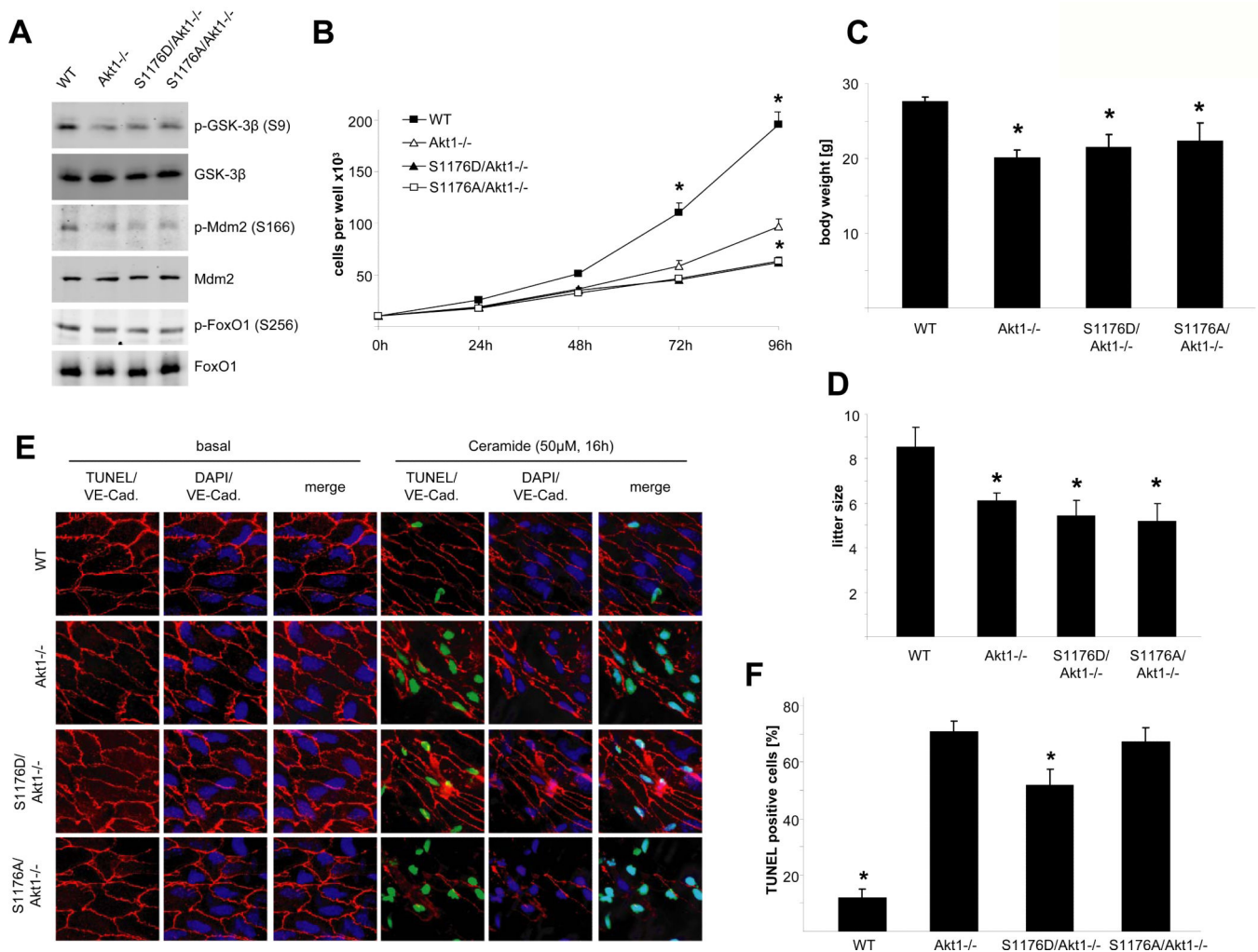
Fig. 2.
eNOS alleles do not rescue impaired growth, proliferation, or litter size in Akt$^{-/-}$ mice. (A)
EC lysates were analyzed for phosphorylation of the Akt targets GSK-3β, Mdm2, and
FoxO1 by Western blot. (B) Proliferation of MLECs from the respective genotypes was
performed. (C) Body weight of 12-week-old mice was analyzed. (D) Litter sizes from 8- to
27-week-old females were measured on the day of birth. (E) Cell survival ex vivo was
analyzed by inducing apoptosis in carotid artery sections with ceramide and subsequent en
face TUNEL staining for apoptotic nuclei (green, TUNEL staining; red, VE-cadherin, used
to delineate the endothelial cell plasma membrane; blue, DAPI). (F) Results from (E) were
quantified by counting TUNEL-positive nuclei out of a total of 100 nuclei. (B and C) $n = 10$;
(D) $n = 6$; (F) $n = 4$; error bars indicate SEM. (B and F) *$P < 0.05$ compared against
Akt1$^{-/-}$; (C and D) *$P < 0.05$ compared to WT by two-way ANOVA.
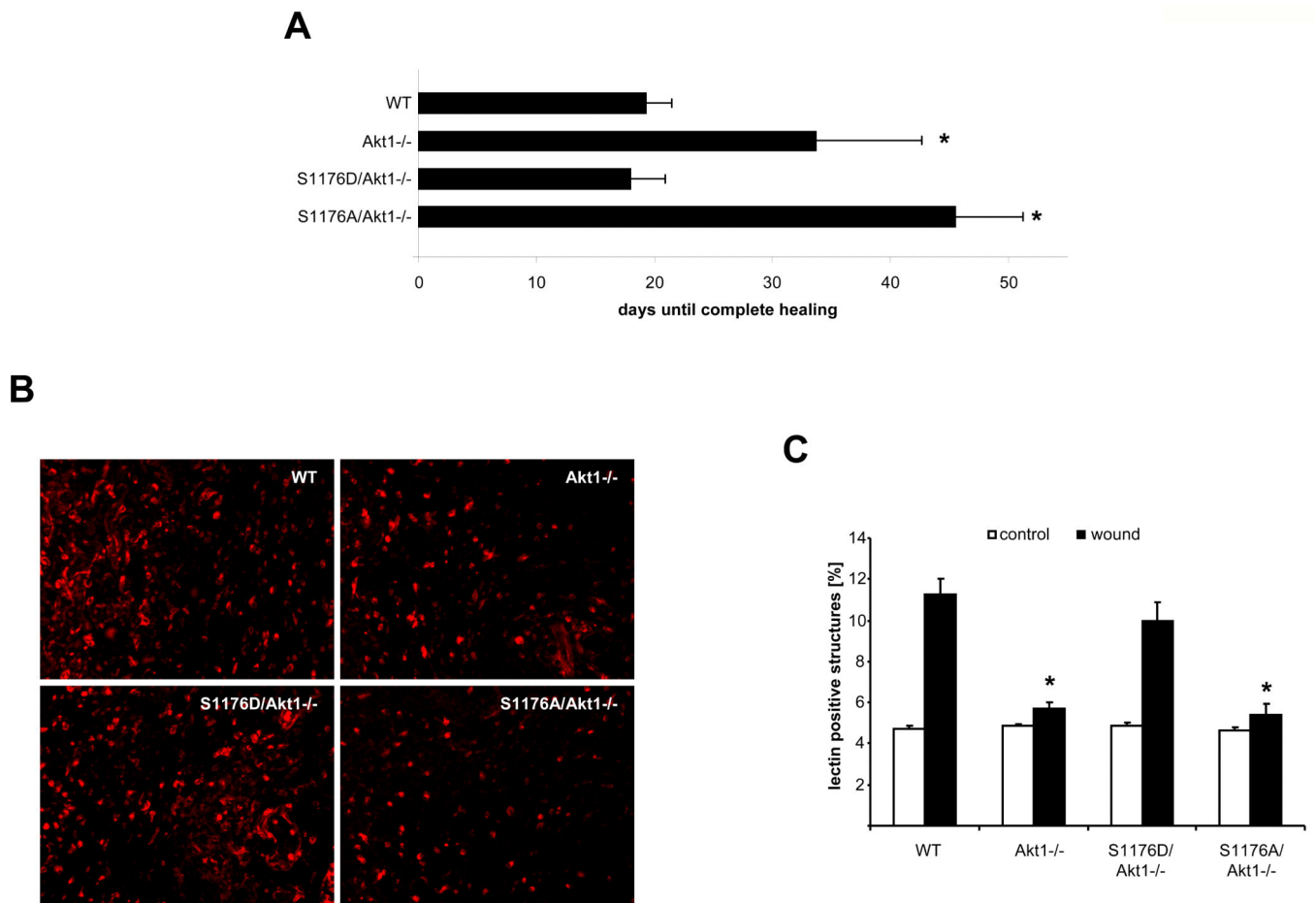
A

B

C

Fig. 3.
Activated eNOS, but not S176A eNOS, rescues impaired wound healing in Akt1-deficient mice. (A) Wound closure time was monitored in mice from all groups. (B) Density of ECs was analyzed by immunofluorescent staining with isolectin B4 (red). (C) Blood vessel density in the wound tissue was quantified with ImageJ software. (A) $n = 5$ mice repeated in two different experiments; (C) $n = 3$ mice per group with five pictures per mouse averaged; (A and C) data are the mean ± SEM.*$P < 0.05$ compared to WT; (C) +$P < 0.05$ compared to wounded WT by two-way ANOVA.
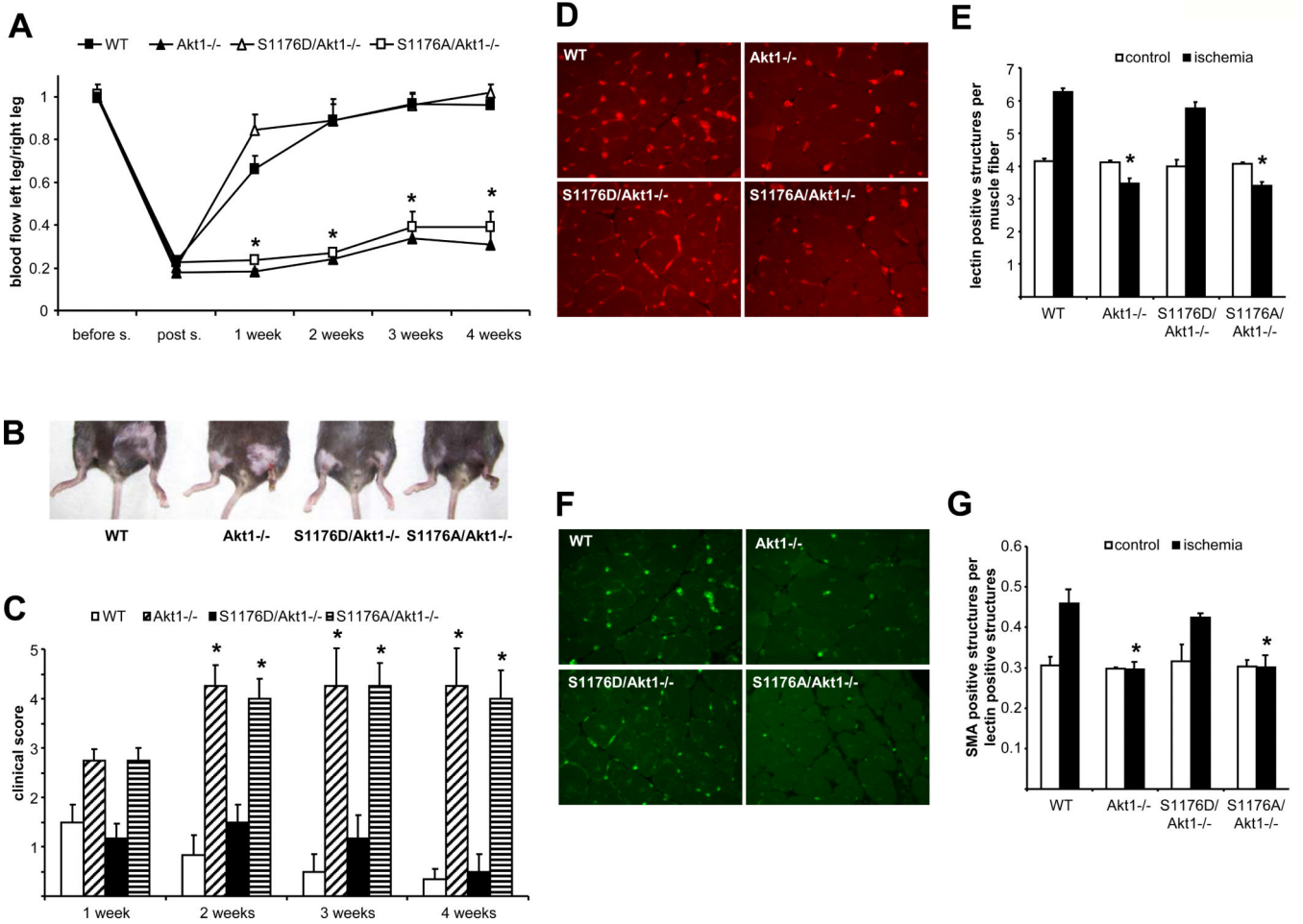
Fig. 4.

Activated eNOS, but not S1176A eNOS, rescues impaired blood flow in Akt1-deficient mice. (A) Hind-limb ischemia was performed in the four groups of mice as described and blood flow in the lower leg was monitored over 4 weeks. (B) Representative pictures of control (left) and ischemic legs (right) after 4 weeks. (C) Clinical score was assessed over 4 weeks. Angiogenic endothelium (D) and pericyte recruitment (F) in ischemic muscle were analyzed by immunofluorescent staining with isolectin B4 or smooth muscle α-actin, respectively, and quantified in (E) and (G). (A and B) $n = 5$ mice per group; (C, E, and G) $n = 4$, five slides were averaged per experiment; data are mean ± SEM. (A and C) *$P < 0.05$ compared to WT and S1176D/Akt1$^{-/-}$; (E and G) *$P < 0.05$ compared to control, $^+P < 0.05$ compared to WT ischemic tissue by two-way ANOVA.
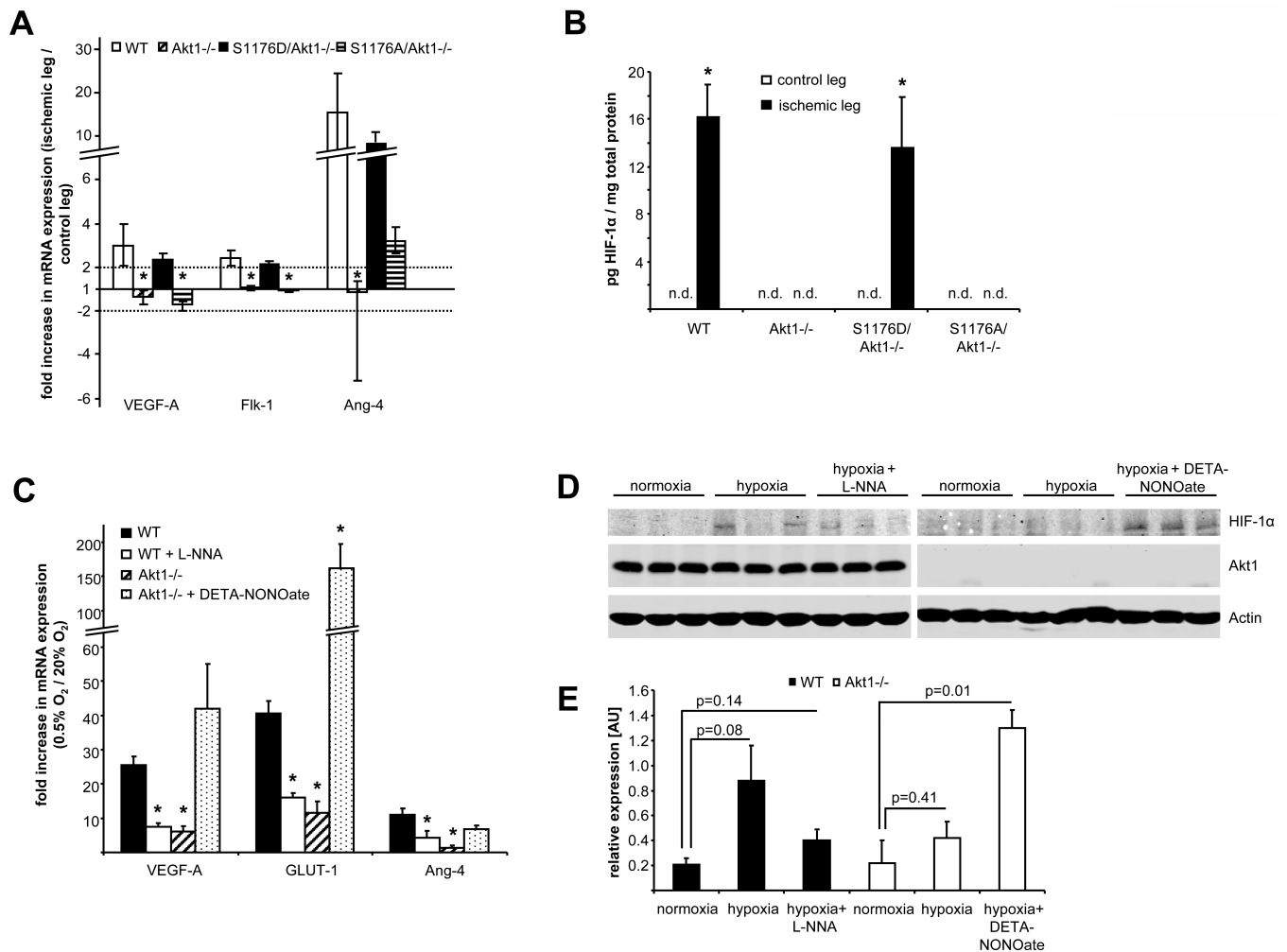
Fig. 5.
Activated eNOS rescues induction of HIF-1α–responsive genes caused by Akt1 deficiency. (A) Mice were subjected to hind-limb ischemia and total RNA prepared for examination of HIF-1α–responsive gene induction by quantitative reverse transcription PCR (qRT-PCR) from gastrocnemic muscles 6 or 24 hours after ischemia. (B) HIF-1α protein in gastrocnemius muscle extracts was quantified 6 hours after ischemia (n.d., not detectable). (C) WT and Akt1−/− MLECs were subjected to 0.5% oxygen for 12 hours in the presence and absence of L-NNA or DETA-NONOate and induction of HIF-1α–responsive genes was analyzed by qRT-PCR. (D) WT and Akt1−/− MLECs were subjected to 0.5% oxygen for 3 hours in the presence and absence of L-NNA or DETA-NONOate. Cell lysates from three independent experiments were analyzed for HIF-1α, Akt1, and β-actin by Western blot. (E) HIF-1α levels from the cell lysates were quantified and expressed relative to actin. (A, B, C, and E) n = 3, error bars indicate SEM. (A) *P < 0.05 compared to WT. (C) *P < 0.05 compared to WT cells. (E) *P < 0.05 compared against normoxia in the respective genotype of cells by two-way ANOVA.